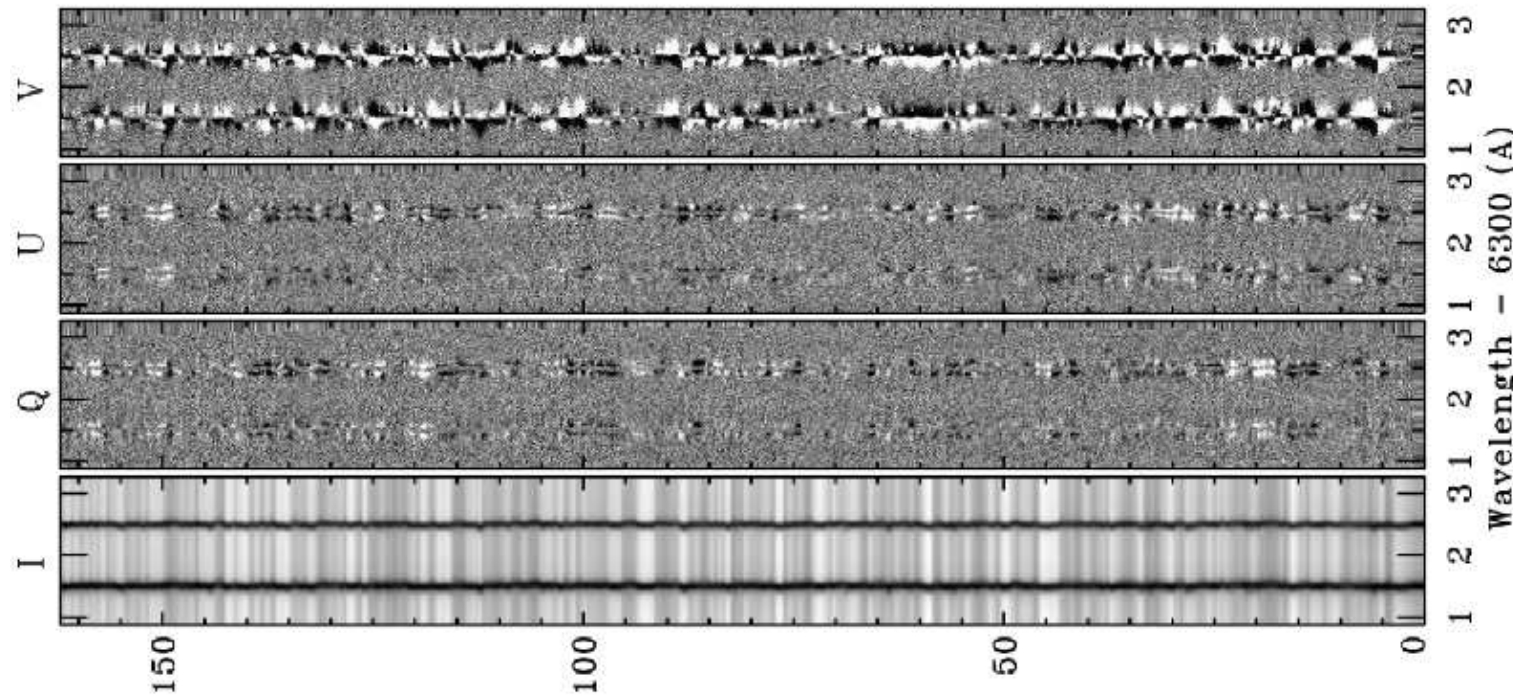


The horizontal magnetic field of the quiet Sun: Numerical simulations in comparison to observations with Hinode

O. Steiner, R. Rezaei, W. Schaffenberger, R. Schlichenmaier, and
S. Wedemeyer-Böhm

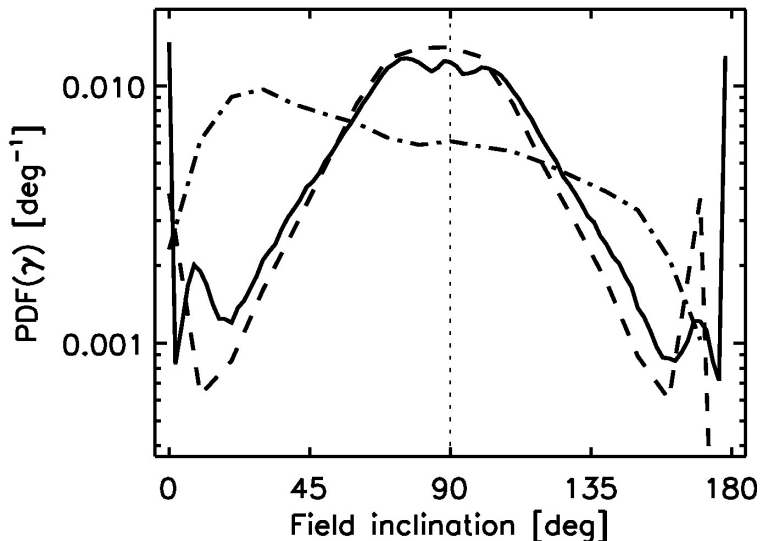
1. Observations



Deep mode *Stokes spectra* with an integration time of 67.2 s and a rms polarization in the continuum of 3×10^{-4} . From a 2-hour time series Lites et al. obtain mean apparent longitudinal and transversal field strengths of $\langle B_{\text{app}}^{\text{L}} \rangle = 11.0 \text{ Mx cm}^{-2}$ and $\langle B_{\text{app}}^{\text{T}} \rangle = 55.3 \text{ Mx cm}^{-2}$. From *Lites et al. 08*

Observations (cont.)

A predominance of horizontally directed magnetic fields in the quiet Sun was also reported by *Orozco Suárez et al. 07* from *HINODE* measurements and by *Harvey et al. 07* from center-to-limb measurements with GONG and SOLIS.



Probability density of the magnetic field inclination in the inter-network. From *Orozco Suárez et al. 07*.

Ishikawa et. al. 08 detected transient horizontal magnetic fields in plage regions with SOT/Hinode

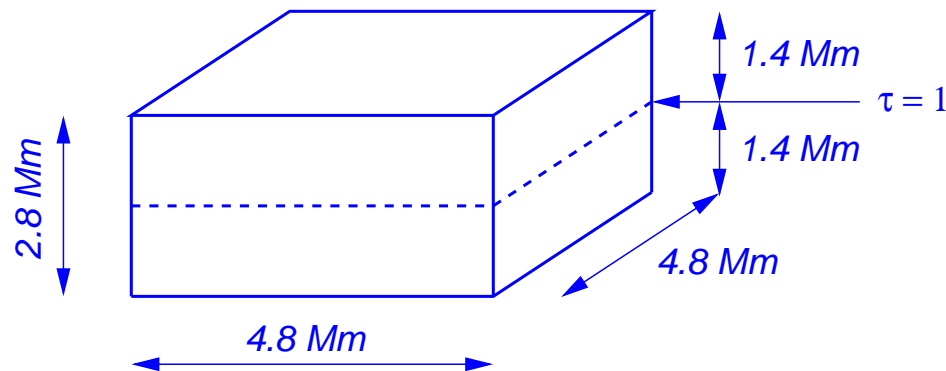
Previously, *Meunier et al. 1998* and *Martinez Pillet et al. 97* reported observations of weak and strong horizontal field in quiet Sun regions.

Questions:

- Do simulations of the surface layers of the Sun intrinsically produce horizontal magnetic fields ?
- If yes, how do they originate ?
- How does the polarimetric signal from simulations compare to measurements ?

2. Numerical simulations

Three-dimensional computational domain encompassing the integral layers from the upper convection zone to the middle chromosphere.

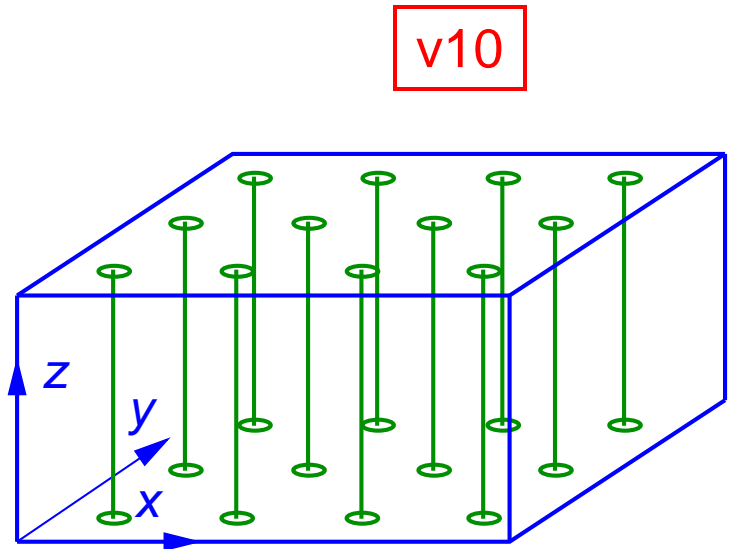


Top boundary located sufficiently high for not to unduly tamper the photospheric layers, from where the polarimetric signals measured with SOT/Hinode originate.

Two simulation runs, which significantly differ in their initial and boundary conditions for the magnetic field.

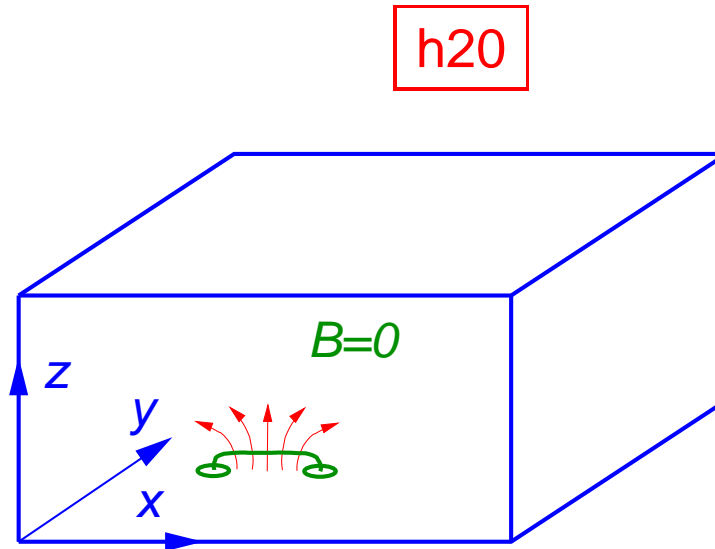
Numerical simulations (cont.)

Different initial states and boundary conditions for the magnetic field



Initial homogeneous, vertical, unipolar
B-field of 10 G.

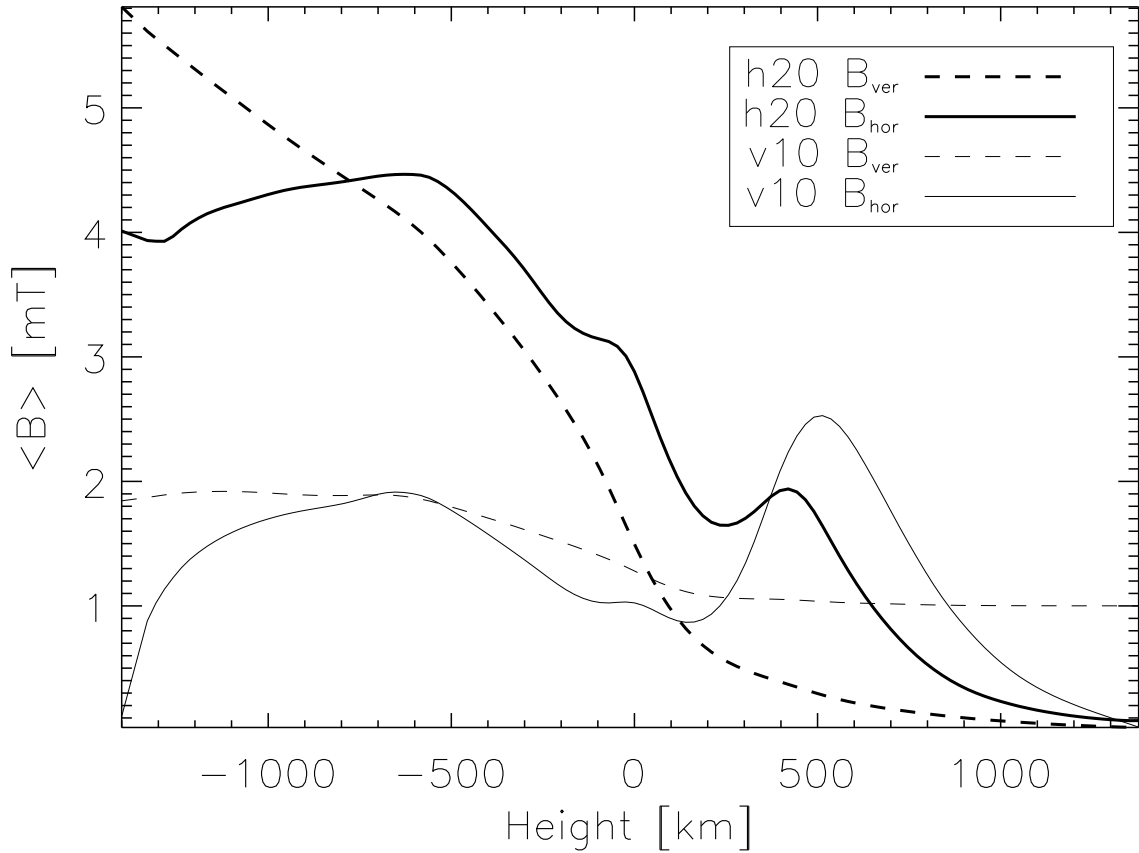
$$B_{x,y} = 0; \quad \partial B_z / \partial z = 0$$



Fluid that enters the simulation domain
from below carries horizontal magnetic
field of $B_x = 20$ G.
 $\partial B_{x,y,z} / \partial z = 0$

Numerical simulations (cont.)

Horizontally and temporally averaged absolute vertical and horizontal magnetic flux density as a function of height for both runs.



$$\langle B_{\text{hor}} \rangle = \langle \sqrt{B_x^2 + B_y^2} \rangle$$

run v10:

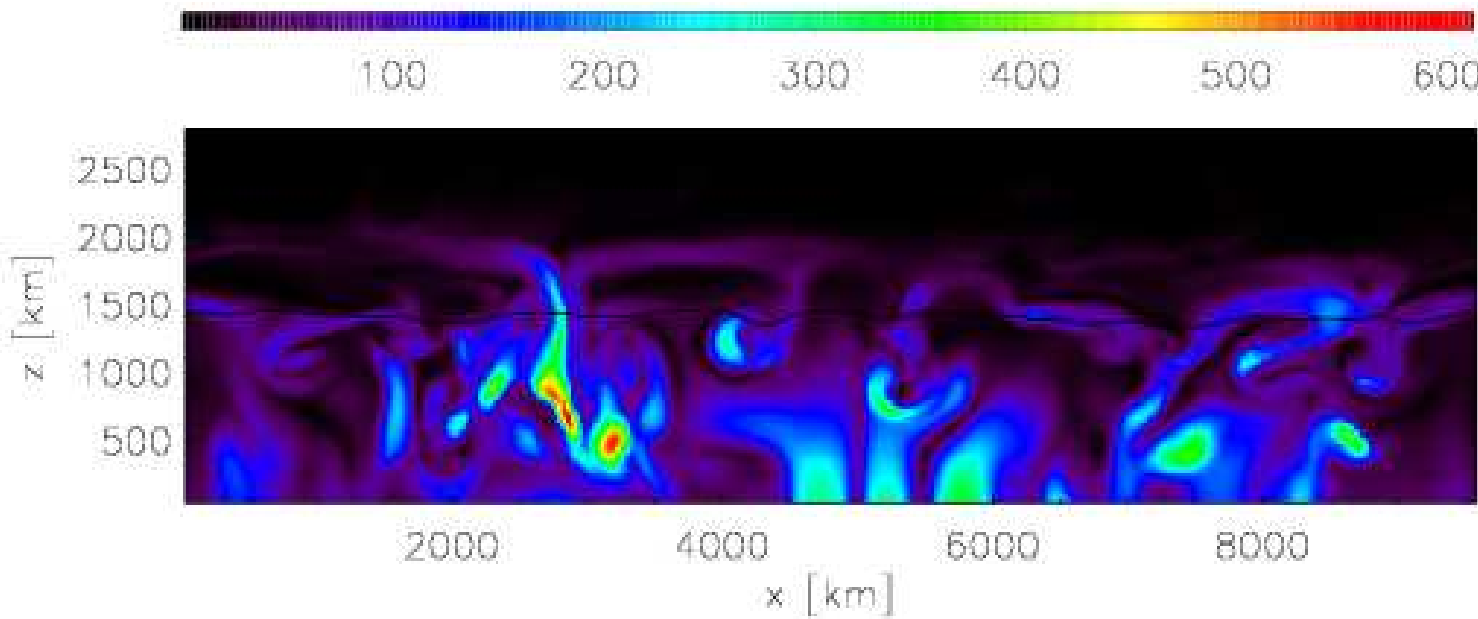
$$\langle B_{\text{hor}} \rangle / \langle |B_{\text{ver}}| \rangle (500 \text{ km}) = 2.5$$

run h20:

$$\langle B_{\text{hor}} \rangle / \langle |B_{\text{ver}}| \rangle (420 \text{ km}) = 5.6$$

Numerical simulations (cont.)

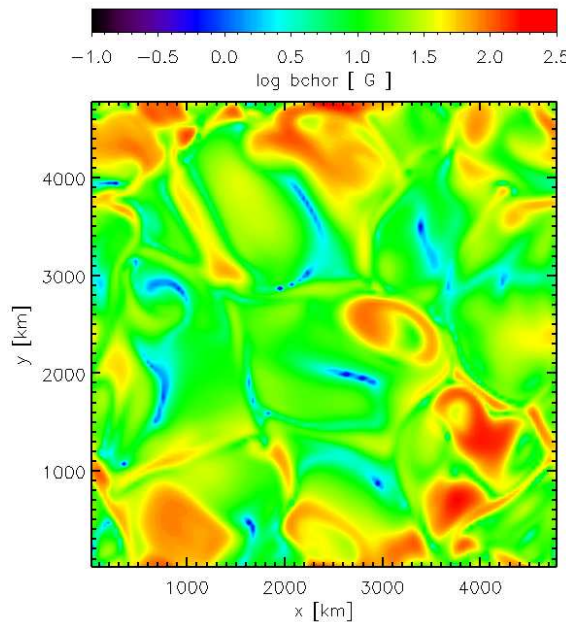
Vertical section through computational domain...



... shows horizontal sheets of enhanced magnetic field strength in the upper photosphere — *the seething magnetic field*.

Numerical simulations (cont.)

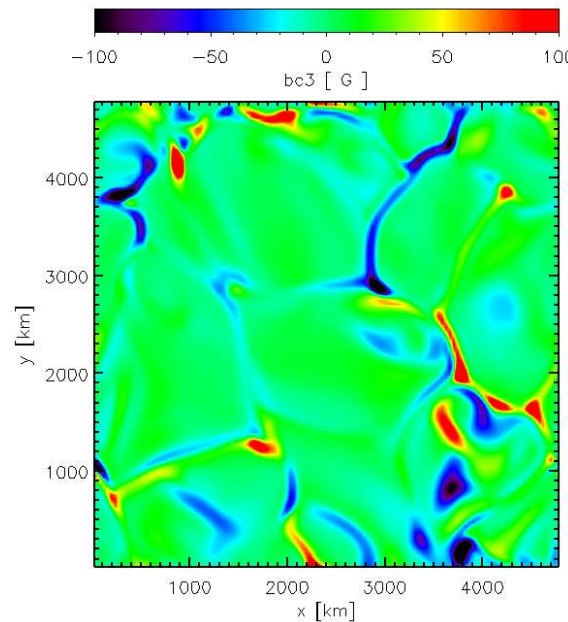
Snapshot of B_{hor} , B_{ver} , and the continuum intensity at 630 nm from *run h20* in the horizontal section of $\langle \tau_{500 \text{ nm}} \rangle = 1$.



B_{hor}

area fraction with

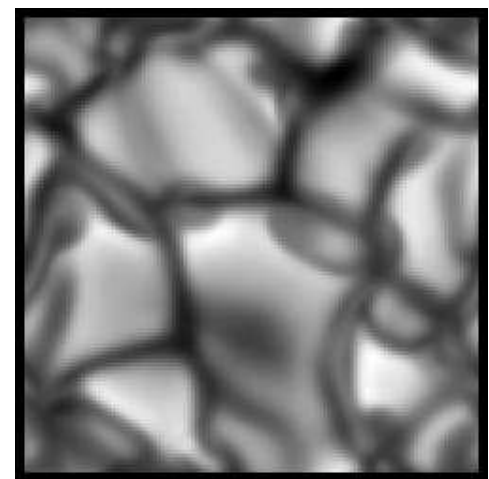
$$B_{\text{hor}} > 5 \text{ mT} = 17\%$$



B_{ver}

area fraction with

$$B_{\text{ver}} > 5 \text{ mT} = 2.2\%$$



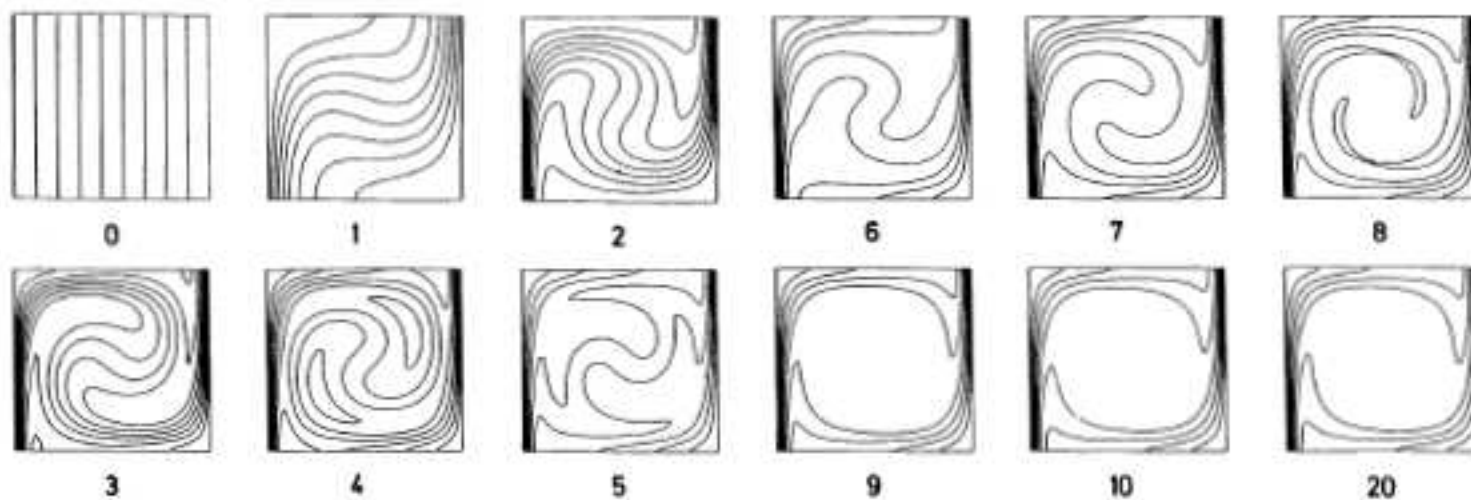
$I_{630 \text{ nm}}$

$$v_z(\langle \tau_{500 \text{ nm}} \rangle = 1)$$

Movie

Numerical simulations (cont.)

The horizontal field can be considered a consequence of the *flux expulsion process* (Parker, 1963; Weiss, 1964): in the same way as magnetic flux is expelled from the granular interior to the intergranular lanes, it also gets pushed to the middle and upper photosphere by overshooting convection, where it tends to form a layer of horizontal field.



From *Galloway & Weiss, 1981*

3. The Poynting flux

Equation for the total energy:

$$\frac{\partial e}{\partial t} + \nabla \left[(h + \frac{1}{2}v^2)\rho \mathbf{v} + \mathbf{S} \right] - \mathbf{g} \cdot \mathbf{v} = 0 ,$$

where

$$e = \rho \epsilon + \frac{1}{2} \rho v^2 + \frac{B^2}{2\mu} , \quad h = \epsilon + \frac{p}{\rho} ,$$

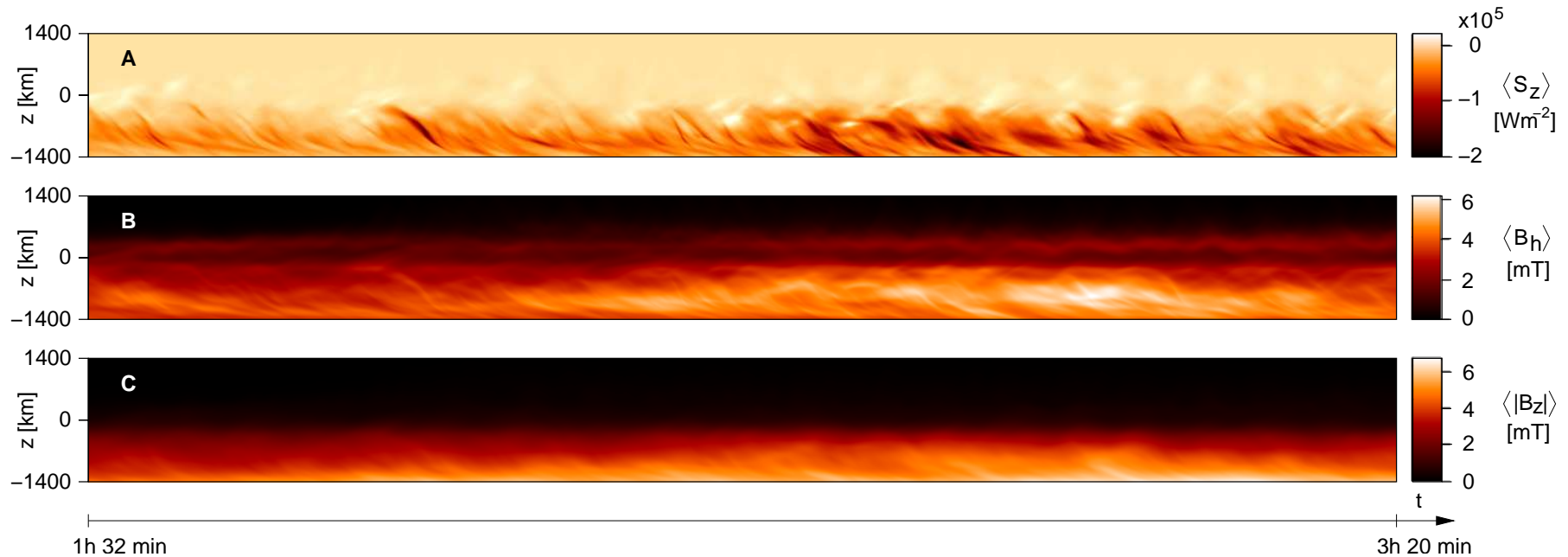
and

$$\mathbf{S} = \frac{1}{4\pi} (\mathbf{B} \times (\mathbf{v} \times \mathbf{B}))$$

The Poynting flux (cont.)

Vertically directed Poynting flux, $\langle S_z \rangle$, $\langle B_{\text{hor}} \rangle$, and $\langle |B_z| \rangle$ as a function of time and height in the atmosphere.

$$\mathbf{S} = \frac{1}{4\pi}(\mathbf{B} \times (\mathbf{v} \times \mathbf{B}))$$

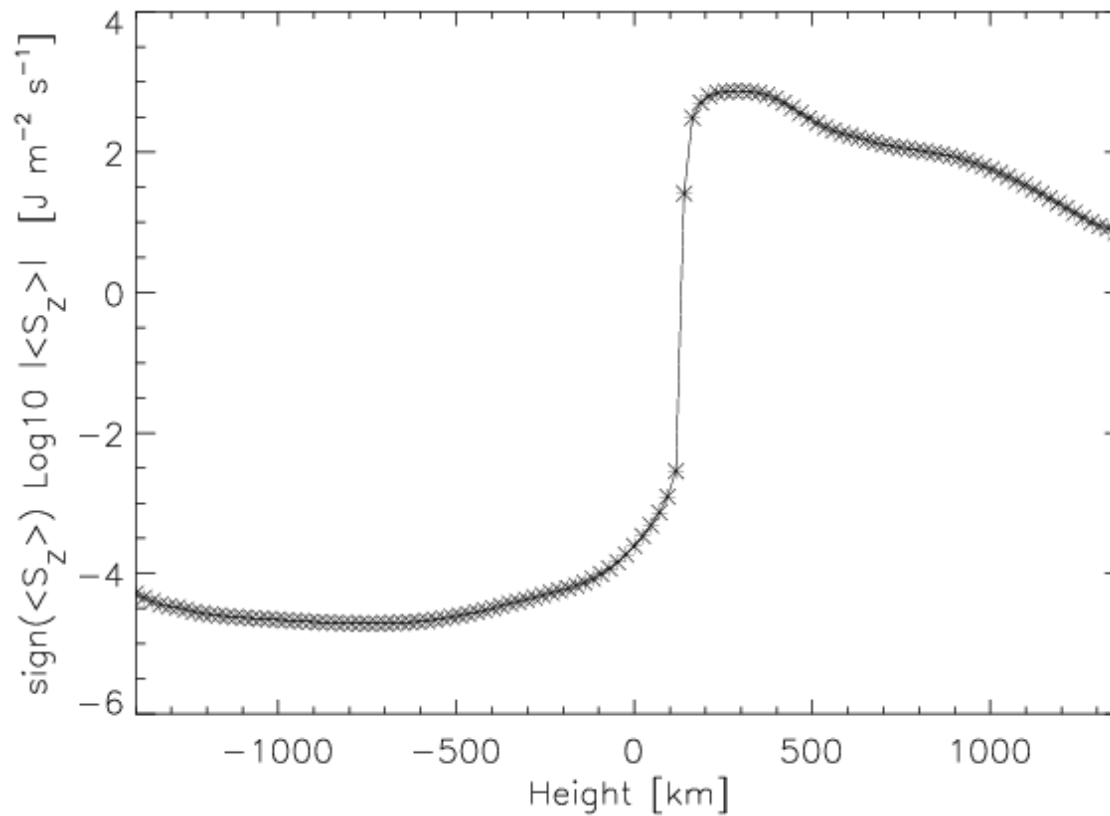


From Steiner, Rezaei, Schaffenberger, & Wedemeyer-Böhm, 2008, ApJ 680, L85-L88

The surface of optical depth unity is a separatrix for the vertically directed Poynting flux.

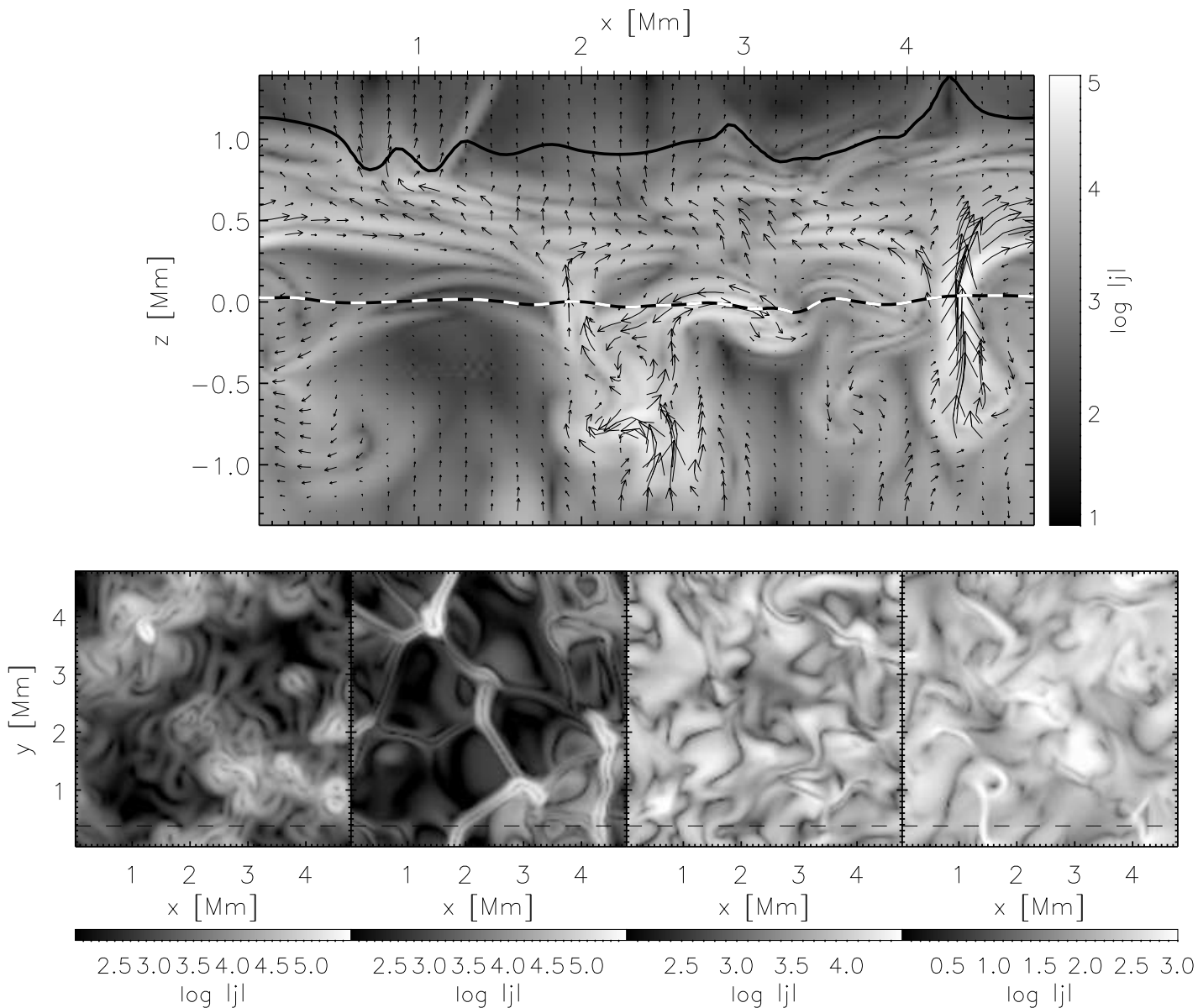
The Poynting flux (cont.)

Vertically directed Poynting flux, $\langle S_z \rangle$, as a function of height in the atmosphere.



The temporal average of $\langle S_z \rangle$ is maximal $7.4 \times 10^2 \text{ Wm}^{-2}$ (at 200 km) and minimal $-5.2 \times 10^4 \text{ Wm}^{-2}$ (at -800 km). For comparison: the chromospheric radiative energy loss is about $4.3 \times 10^3 \text{ Wm}^{-2}$.

The Poynting flux (cont.)



Logarithmic current density, $\log |j|$, in a vertical cross section (top panel) and in four horizontal cross sections in a depth of 1180 km below, and at heights of 90 km, 610 km, and 1310 km above the average height of optical depth unity from left to right, respectively. The arrows in the top panel indicate the *magnetic field* strength and direction.

From Schaffenberger, Wedemeyer-Böhm, Steiner, and Freytag, 2006, ASP Conf. Ser., Vol. 354, p. 345

4. Polarimetry

- We synthesized the Stokes profiles of both 630 nm Fe I spectral lines observed by the Hinode SP with a spectral sampling of 2 pm.
- We then compute

$$V_{\text{tot}} = \frac{\int_{\lambda_b}^{\lambda_0} V(\lambda) d\lambda - \int_{\lambda_0}^{\lambda_r} V(\lambda) d\lambda}{I_c} ,$$

and

$$Q_{\text{tot}} = \frac{\int Q(\lambda) Q_{\text{mask}}(\lambda) d\lambda}{I_c} ,$$

- We subject these quantities to exactly the same calibration procedure for conversion to apparent flux density as was done with the real data by Lites et al. 08.

Polarimetry (cont.)

Lites et al. (2007) found from the deep mode series

$$\frac{\langle B_{\text{app}}^T \rangle}{\langle B_{\text{app}}^L \rangle} = \frac{55.3 \text{ Mx cm}^{-2}}{11.0 \text{ Mx cm}^{-2}} \approx 5.$$

From the synthesized Stokes profiles and application of the SOT-PSF we find

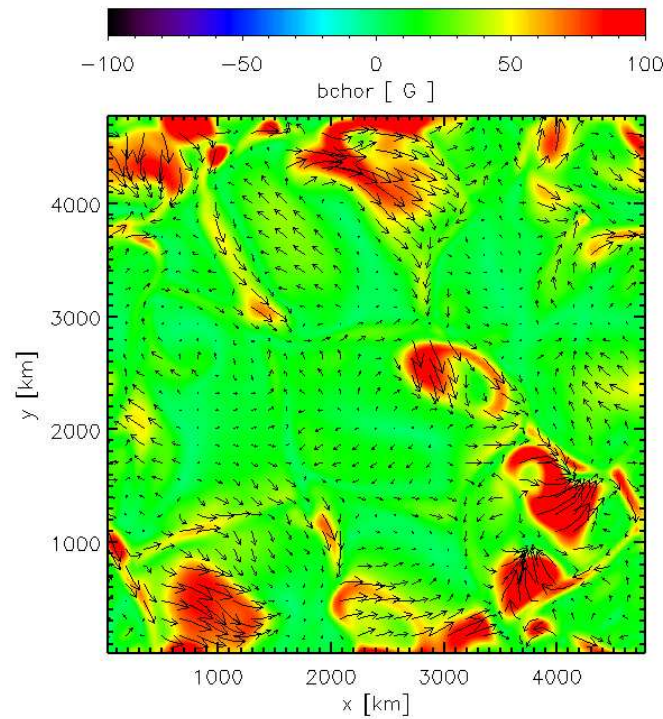
$$\frac{\langle B_{\text{app}}^T \rangle}{\langle B_{\text{app}}^L \rangle} = \begin{cases} 10.4 \text{ G}/6.6 \text{ G} = 1.6 & \text{for run } v10 \\ 21.5 \text{ G}/5.0 \text{ G} = 4.3 & \text{for run } h20 \end{cases}.$$

without the PSF we got

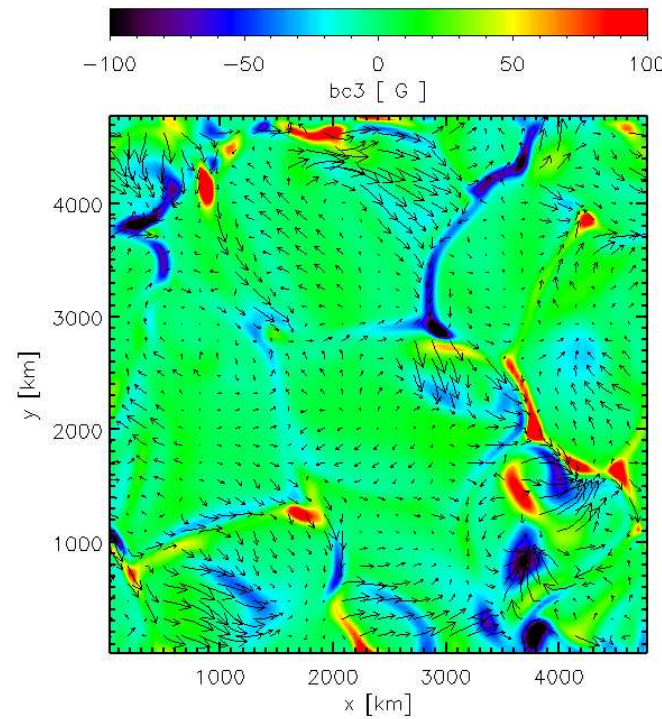
$$\frac{\langle B_{\text{app}}^T \rangle}{\langle B_{\text{app}}^L \rangle} = \begin{cases} 11.5 \text{ G}/7.5 \text{ G} = 1.5 & \text{for run } v10 \\ 24.8 \text{ G}/8.8 \text{ G} = 2.8 & \text{for run } h20 \end{cases}.$$

Polarimetry (cont.)

The vertical field component is more subject to apparent flux cancellation than the horizontal component, because



B_{hor}

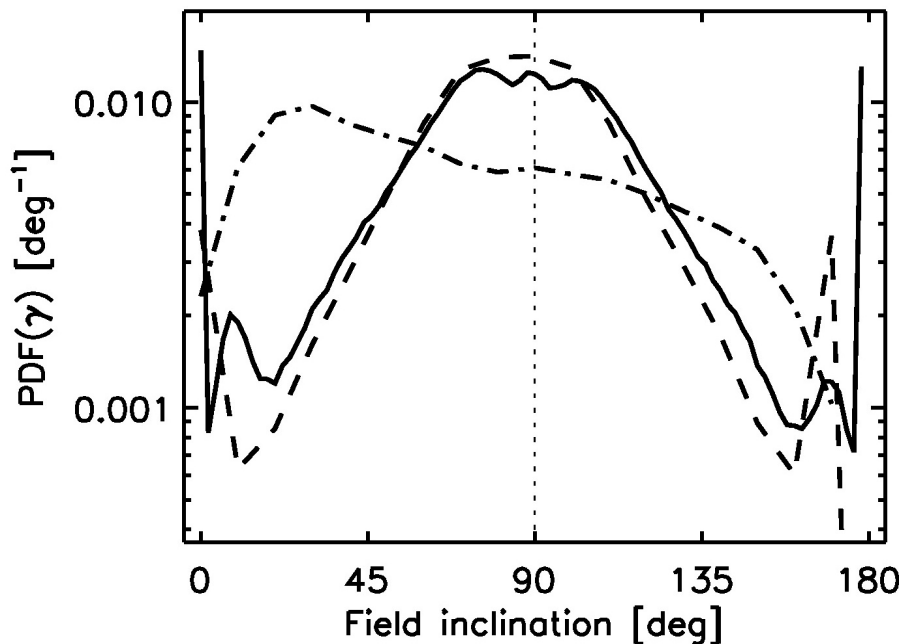


B_{ver}

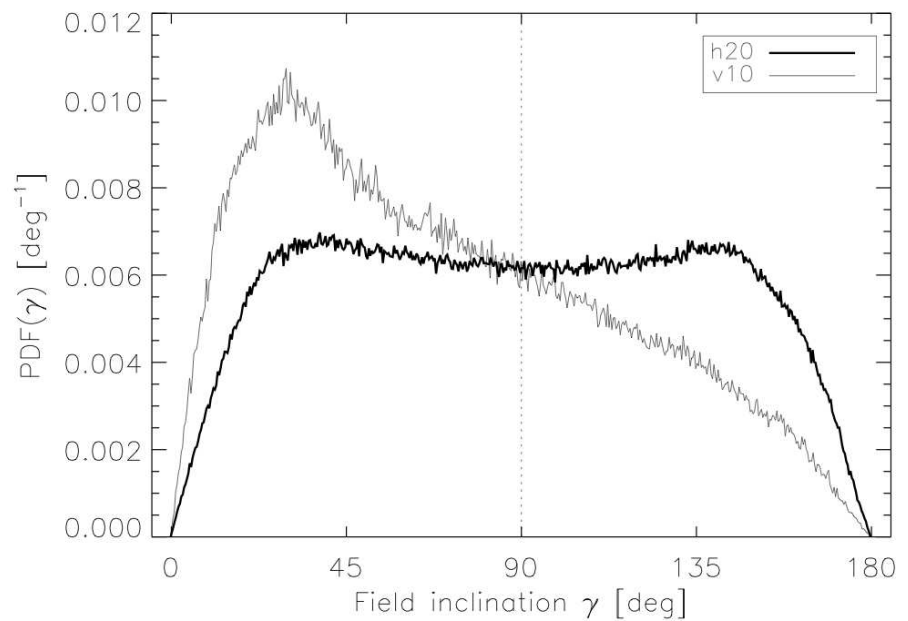
..... the vertical field component has smaller scales and higher intermittency than the horizontal component.

Polarimetry (cont.)

Probability density functions of the magnetic field inclination from *observations of Orozco Suárez et al. (2007)* and simulations



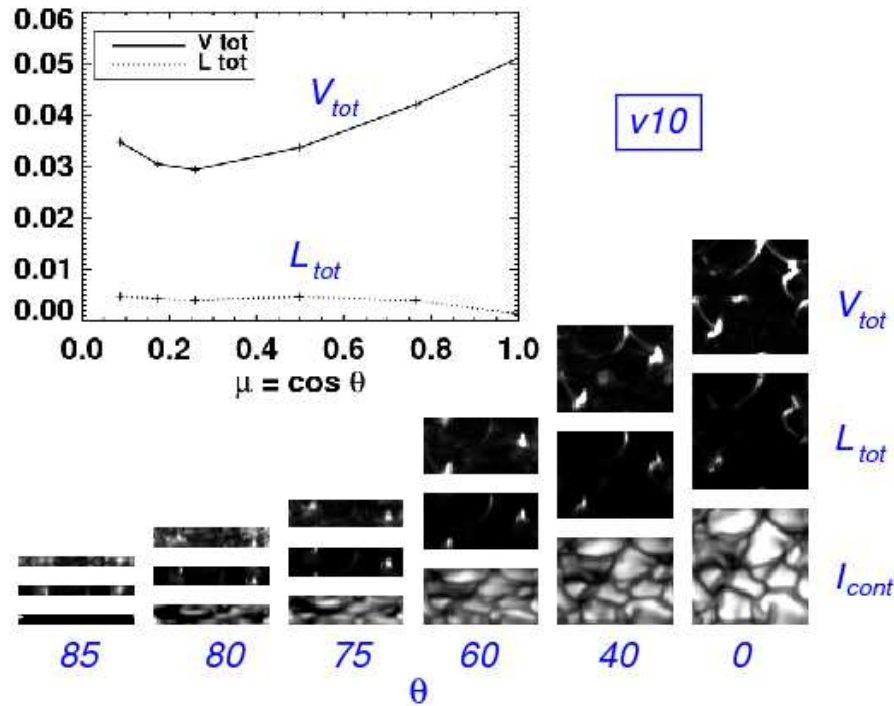
Solid and dashed PDFs represent all pixels in the FOV and the IN regions, respectively. Dot-dashed curve shows PDFs from magnetoconvection *simulations* with a mean flux density of 10 Mx cm^{-2} from Vögler et al. (2005).



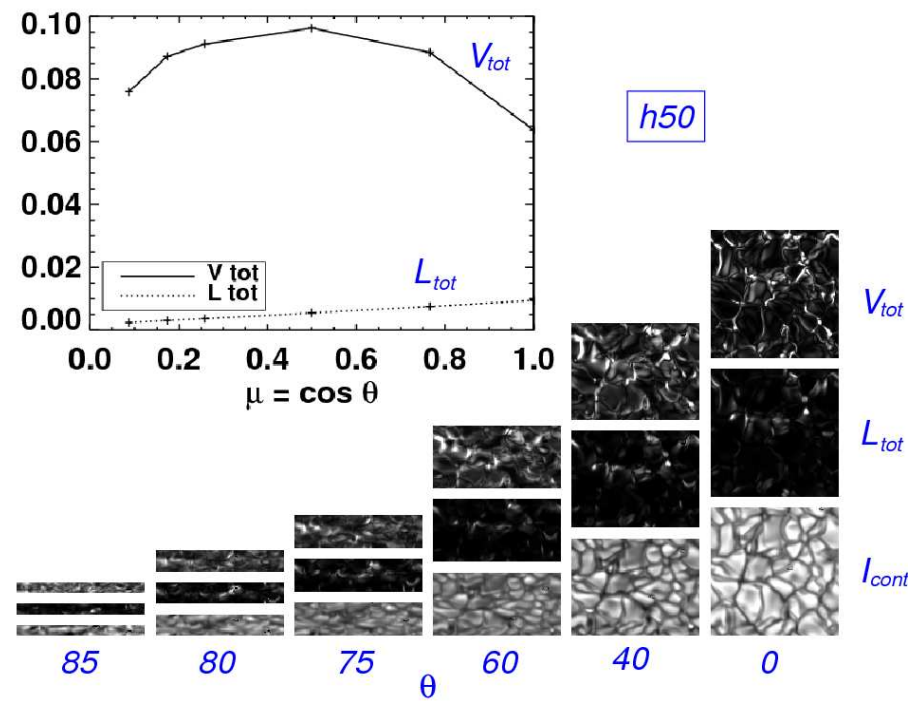
PDF of inclination angle for *simulation* runs h20 and v10 of Steiner et al. (2008).

Polarimetry (cont.)

Center-to-limb variation



Vertical field dominates in the low photosphere
Horizontal field dominates in the upper photosphere



Horizontal field dominates throughout the photosphere

Conclusions

- Simulations intrinsically produce a predominantly horizontally directed magnetic field in the upper photosphere.
- The horizontal field is a product of magnetic flux expulsion by the granular flow.
- Overshooting convection and convective plumes act in a way to make the solar surface a separatrix for the vertical Poynting flux. Above this surface S_z is positive, below it negative.
- The polarimetric response in the FeI line pair at 630 nm compares well with the Hinode observations at disk center.
- The polarimetric center-to-limb behaviour seems to be quite sensitive on the details of the simulation.

Table of content

1. Observations
2. Numerical simulations
3. The Poynting flux
4. Polarimetry

Conclusions

Reference

References

- Galloway, D. J. and Weiss, N. O.: 1981 ApJ 243, 945
- Harvey, J. W., Branston, D., Henney, C. J. and Keller, C.U.: 2007, *Seething horizontal magnetic fields in the quiet solar photosphere*, ApJ 659, L177-L180
- Ishikawa, R., Tsuneta, S., Ichimoto, K., Isobe, H., Katsukawa, Y., Lites, B. W., Nagata, S., Shimizu, T., Shine, R. A., Suematsu, Y., Tarbell, T. D., & Title, A. M.: 2008, *Transient horizontal magnetic fields in solar plage regions*, A&A 481, L25-L28
- Lites, B. W., Kubo, M., Socas-Navarro, H., Berger, T., Frank, Z., Shine, R., Tarbell, T., Title, A., Ichimoto, K., Katsukawa, Y., Tsuneta, S., Suematsu, Y., Shimizu, T., and Nagata, S.: 2008, *The Horizontal Magnetic Flux of the Quiet-Sun Internetwork as Observed with the Hinode Spectro-Polarimeter*, ApJ 672, 1237-1253
- Martinez Pillet, V., Lites, B. W., Skumanich, A.: 1997, ApJ 474, 810
- Meunier, N., Solanki, S. K., Livingston, W. C.: 1998, A&A 332, 771
- Orozco Suárez, D., Bellot Rubio, L. R., del Toro Iniesta, J. C., Tsuneta, S., Lites, B. W., Ichimoto, K., Katsukawa, Y., Nagata, S., Shimizu, T., Shine, R. A., Suematsu, Y., Tarbell, T. D., & Title, A. M.: 2007, *Quiet-Sun internetwork magnetic fields from the inversion of HINODE measurements*, ApJ 670, L61-L64

References

Parker, E. N.: 1963, ApJ 138, 552

Rezaei, R., Steiner, O., Wedemeyer-Böhm, Schlichenmaier, R., Schmidt, W., and Lites, B.W.: 2008, *Hinode observations reveal boundary layers of magnetic elements in the solar photosphere*, A&A 476, L33-L36

Schaffenberger, W., Wedemeyer-Böhm, S., Steiner, O., and Freytag, B.: 2005, *Magnetohydrodynamic simulation from the convection zone to the chromosphere*, in Chromospheric and Coronal Magnetic Fields, D. Innes, A. Lagg, S.K. Solanki, and D. Danesy (eds.), ESA Publication, SP-596

Schüssler, M., & Vögler, A.: 2008, *Strong horizontal photospheric magnetic field in a surface dynamo simulation*, A&A 481, L5-L8

Schaffenberger, W., Wedemeyer-Böhm, S., Steiner, O., and Freytag, B.: 2006, *Holistic MHD-simulation from the convection zone to the chromosphere*, in Solar MHD: Theory and Observations – a High Spatial Resolution Perspective, J. Leibacher, H. Uitenbroek, & R.F. Stein (eds.), ASP Conference Series

References

Steiner, O., Rezaei, R., Schaffenberger, W., and Wedemeyer-Böhm: 2005, *Strong horizontal internetwork magnetic field: numerical simulations in comparison to observations with Hinode*, ApJ 680, L85-L88

Wedemeyer-Böhm, S.: 2008, *Point spread functions for the Solar Optical Telescope onboard Hinode*, A&A, submitted

Weiss, N. O.: 1964, Phil. Trans. R. Soc. London A 256, 99